AGU PUBLICATIONS

Geophysical Research Letters

RESEARCH LETTER
10.1002/2017GL076574

Key Points:
- Salinification has occurred in the South China Sea from late 2012 to the present
- Both surface freshwater forcing and horizontal advection through the Luzon Strait contribute to the salinification
- Sharp fall in precipitation and enhanced Luzon Strait transport dominated the current intense salinification

Supporting Information:
- Supporting Information S1

Correspondence to:
D. Wang,
dxwang@scsio.ac.cn

Citation:
Zeng, L., Chassignet, E. P., Schmitt, R. W., Xu, X., & Wang, D. (2018). Salinification in the South China Sea since late 2012: A reversal of the freshening since the 1990s. *Geophysical Research Letters*, *45*, 2744–2751. https://doi.org/10.1002/2017GL076574

Received 30 NOV 2017
Accepted 1 MAR 2018
Accepted article online 5 MAR 2018
Published online 23 MAR 2018

Salinification in the South China Sea Since Late 2012: A Reversal of the Freshening Since the 1990s

Lili Zeng[1], Eric P. Chassignet[2], Raymond W. Schmitt[3], Xiaobiao Xu[2], and Dongxiao Wang[1]

[1]State Key Laboratory of Tropical Oceanography, South China Sea Institute of Oceanology, Chinese Academy of Sciences, Guangzhou, China, [2]Center for Ocean-Atmospheric Prediction Studies, Florida State University, Tallahassee, FL, USA, [3]Department of Physical Oceanography, Woods Hole Oceanographic Institution, Woods Hole, MA, USA

Abstract Salinification has occurred in the South China Sea from late 2012 to the present, as shown by satellite Aquarius/Soil Moisture Active Passive data and Argo float data. This salinification follows a 20 year freshening trend that started in 1993. The salinification signal is strongest near the surface and extends downward under the seasonal thermocline to a depth of 150 m. The salinification occurs when the phase of the Pacific Decadal Oscillation switches from negative to positive. Diagnosis of the salinity budget suggests that an increasing net surface freshwater loss and the horizontal salt advection through the Luzon Strait driven by the South China Sea throughflow contributed to this ongoing salinification. In particular, a decrease in precipitation and enhanced Luzon Strait transport dominated the current intense salinification. Of particular interest is whether this salinification will continue until it reaches the previous maximum recorded in 1992.

Plain Language Summary A significant salinification is taking place in the South China Sea starting from late 2012 to the present, as seen in satellite and Argo float data. The temperature, in contrast, exhibits no significant change. The salinification is mainly associated with switches in the Pacific Decadal Oscillation from negative to positive phase from late 2012 to the present. A decrease in precipitation and enhanced Luzon Strait transport dominated the current intense salinification. After a freshening period that lasted 20 years, we are particularly interested in whether the salinification will continue in the future.

1. Introduction

Ocean salinity is an essential measurable indicator of the water cycle (e.g., Curry et al., 2003; Durack & Wijffels, 2010; Munk, 2003; Schmitt, 2008; Schmitt & Blair, 2015; Skliris et al., 2014). Over the past five decades, the tropical Indo-Pacific Ocean has freshened remarkably (Durack et al., 2012) and also exhibited multidecadal variability in salinity. Using surface measurements from 1970 to 2003, Delcroix et al. (2007) documented Pacific Decadal Oscillation (PDO)-like signals in surface salinity in the tropical Pacific and reported first a freshening before the mid-1970s then salinification from the mid-1970s to mid-1990s, and freshening again in the mid-1990s. Since 2004, the freshening in the tropical Indian Ocean was continuously recorded by the international Array for Real-time Geostrophic Oceanography (Argo) project (Du et al., 2015).

The South China Sea (SCS), located between the western Pacific Ocean and the Indian Ocean, has also become fresher over the 1960–2014 time period, with a salinity decrease comparable to the change identified by Durack et al. (2012) in the northwest Pacific. The salinity variations in the SCS are consistent with the changes in the tropical Pacific documented by Delcroix et al. (2007). In situ observations in the SCS show that it became fresher in the 1960s, started to salinify again in 1974, and freshened again from 1993 to 2012 (Zeng, Wang, Xiu, et al., 2016). The low salinity in the SCS in 2012 was the lowest in more than 50 years (Zeng et al., 2014).

Many profiling floats have been deployed in the world ocean since 2000 (Argo, 2000), and they allow us to continuously monitor ocean temperature and salinity in the upper layer in near real time (Roemmich et al., 2009). Available Argo floats entered the SCS mainly through the Luzon Strait (approximately 250 km wide and 2–4 km deep) in 2006, although they provided very limited data until 2008. The launch of the Soil Moisture and Ocean Salinity, Aquarius/SAC-D, and Soil Moisture Active Passive (SMAP) satellites opened a new era for monitoring surface salinity variations (Lagerloef et al., 2012; Nyadjro et al., 2013; Reul et al., 2014). Both series of measurements indicate that there is an ongoing salinification in the SCS since late 2012 when the lowest salinity was recorded (Zeng et al., 2014), and we examine here the contribution of atmospheric and oceanic processes to this salinification.

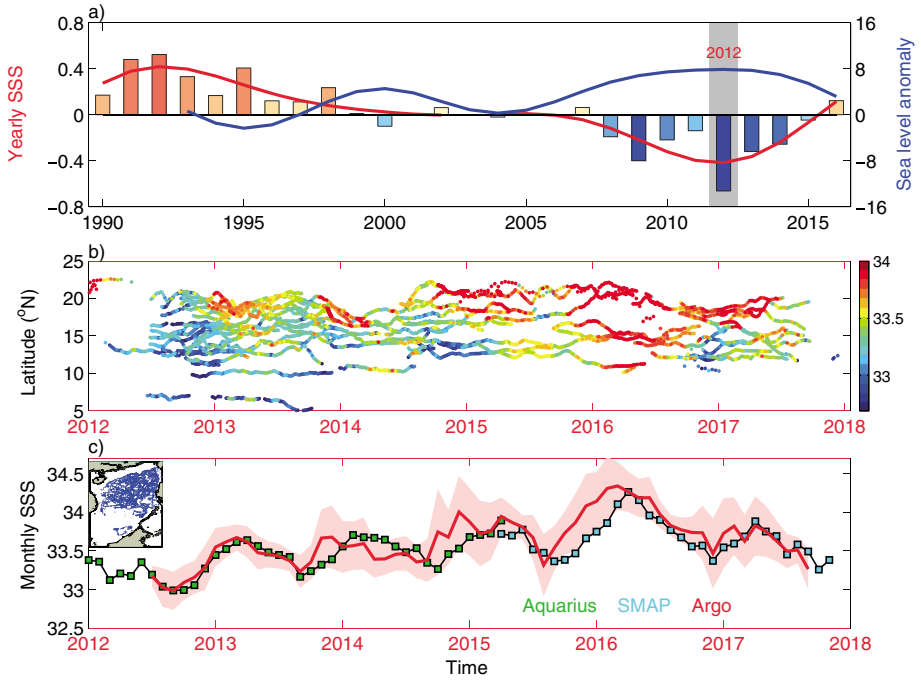

Figure 1. (a) Time series of yearly surface salinity anomalies (positive salinity anomaly: red bars; negative salinity anomaly: blue bars) in the SCS from updated South China Sea Physical Oceanographic Data Set 14. The low-frequency curve of surface salinity anomaly (red) and sea level (blue) represents the 7 year filtered values. The gray shaded area indicates turning point year in 2012. (b) Latitude-time distributions of Argo surface salinity (taken as an average of salinity above 10 m) from 2012 to September 2017. Locations of the Argo floats are shown in the inset of (c). (c) Time series of basin-average monthly mean surface salinity from Aquarius (green squares) and Soil Moisture Active Passive (SMAP) (blue squares) and Argo floats (red line, the Argo sea surface salinity (SSS) is taken as an average of salinity above 10 m) from 2012 to 2017. Calculations are made if more than 10 Argo samples in each month.

2. Data

A total of 9,962 Argo profiles from January 2012 to December 2017 in the SCS and adjacent northwestern Pacific was available to document the recent salinification after quality control procedures. In addition to Argo floats, we also used the South China Sea Physical Oceanographic Data Set 14 (Zeng, Wang, Chen, et al., 2016) and sea surface salinity (SSS) from Aquarius version 3.0 (Lagerloef et al., 2010) and SMAP version 3.0 (Fore et al., 2016) monthly gridded Level-3 products. Because of the radio frequency interference on pixels near the coastline and shelf areas, Aquarius and SMAP salinities in areas shallower than 200 m were removed.

To examine the relative importance of the atmospheric freshwater forcing and of oceanic salinity advection, evaporation, precipitation, and ocean current data sets are also analyzed. The evaporation data are taken from the Objectively Analyzed air-sea Fluxes (Yu & Weller, 2007). The precipitation product is from the Tropical Rainfall Measuring Mission (Huffman et al., 2007). In addition to near-surface currents (averaged over the top 30 m) estimated by Ocean Surface Current Analysis Real-time (OSCAR) (Bonjean & Lagerloef, 2002), we use horizontal velocities at different depths from the Hybrid Coordinate Ocean Model (HYCOM) reanalysis system (Chassignet et al., 2009). While the variability of the HYCOM monthly zonal current within the Luzon Strait (along the 120.5°E) is slightly higher than OSCAR currents (Figure S1a in the supporting information, the standard deviation between them is 0.07 m/s); the HYCOM results are in excellent agreement with an acoustic Doppler current profiler measurements taken from September to December 2015 provided by the South China Sea Institute of Oceanology (Figure S2). To understand the link to atmospheric forcing, the PDO index and the Niño3 index are also used.

3. Results

3.1. Salinification Observed in Argo and Aquarius/SMAP Data From 2012 to the Present

We start with the surface salinity anomaly since the 1990s (Figure 1a). The salinity anomaly is defined as the yearly mean salinity minus the average over the period 1960 to 2016. The SCS started to freshen in 1993 (Zeng, Wang, Xiu, et al., 2016), reaching a salinity minimum in 2012 that has been reported as the lowest

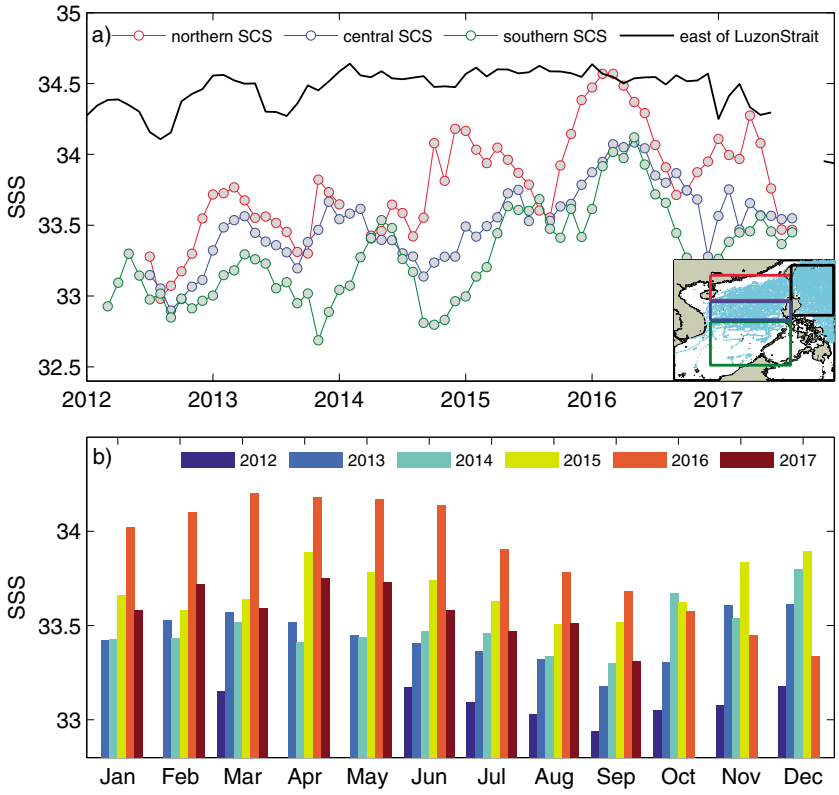

Figure 2. (a) Time series of box-average monthly mean surface salinity from Argo floats within four regions (east of Luzon Strait (121–127°E, 15–25°N): black; northern South China Sea (SCS) (110–121°E, 18–23°N): red; central SCS (110–121°E, 14–18°N): blue; southern SCS (110–121°E, 5–14°N): green; SCS (105–121°E, 5–25°N): gray) from 2012 to September 2017. Calculations are made if more than 10 samples in each month for each region. Locations of the Argo floats and four selected areas used for spatial averages are shown in the inset. (b) Histograms of basin-average (105–121°E, 5–25°N) yearly mean surface salinity in each month from Argo floats. SSS = sea surface salinity.

salinity on record in more than 50 years (Zeng et al., 2014). This freshening period lasted for about 20 years, with a decrease of about 1.0 psu. Accompanying this significant freshening in the SCS, there was an increase in sea surface height during the 1990s and 2000s, which has been widely discussed (Cheng et al., 2016; Rong et al., 2007). But the situation after 2012 is very different, with a drop in sea level and an increase in SSS. Thus, 2012 appears to be a turning point for salinity.

After 2008, an increasing number of Argo floats entered the SCS and therefore provided an opportunity for monitoring the salinity changes over the water column. Although the sampling is uneven, with more samples in the north and fewer in the south, it is clear that near-surface waters at all latitudes do become substantially saltier (Figure 1b). Here the Argo SSS is taken as an average of salinity above 10 m, typically from 5 to 10 m. Figure 1c summarizes the basin-average (105–121°E, 5–25°N) monthly mean SSS values from Argo floats and Aquarius/SMAP surface salinity. The Aquarius surface salinity data, after correction for the systematic bias of 0.45 psu (Zeng et al., 2014), agree well with Argo near-surface observations during the satellite life span from August 2011 to May 2015. The subsequent SMAP salinity data, from April 2015 to November 2017, also agree well with Argo observations. These data clearly show a strong salinification. The monthly mean Argo SSS increased from 32.98 psu in September 2012 to 34.30 psu in March 2016 and come down somewhat following the peak. It is noteworthy that the rate of yearly surface salinity increase (from 33.12 psu in 2012 to 33.99 psu in 2016, or 0.17 psu/yr) is about 8 times higher than the 1974–1993 salinification trend (of 0.02 psu/yr) reported in Zeng, Wang, Xiu, et al. (2016).

The increase in surface salinity inferred from Figure 1b is not homogenous. In order to see the salinity variability in different regions, four areas are selected: east of the Luzon Strait (121–127°E, 15–25°N), the northern SCS (110–121°E, 18–23°N), the central SCS (110–121°E, 14–18°N), and the southern SCS (110–121°E, 5–14°N). The surface salinities averaged in the three regions of the SCS all show an increasing trend, largest in the northern basin and decreasing southward (Figure 2a). Interestingly, the SCS salinity increases faster than

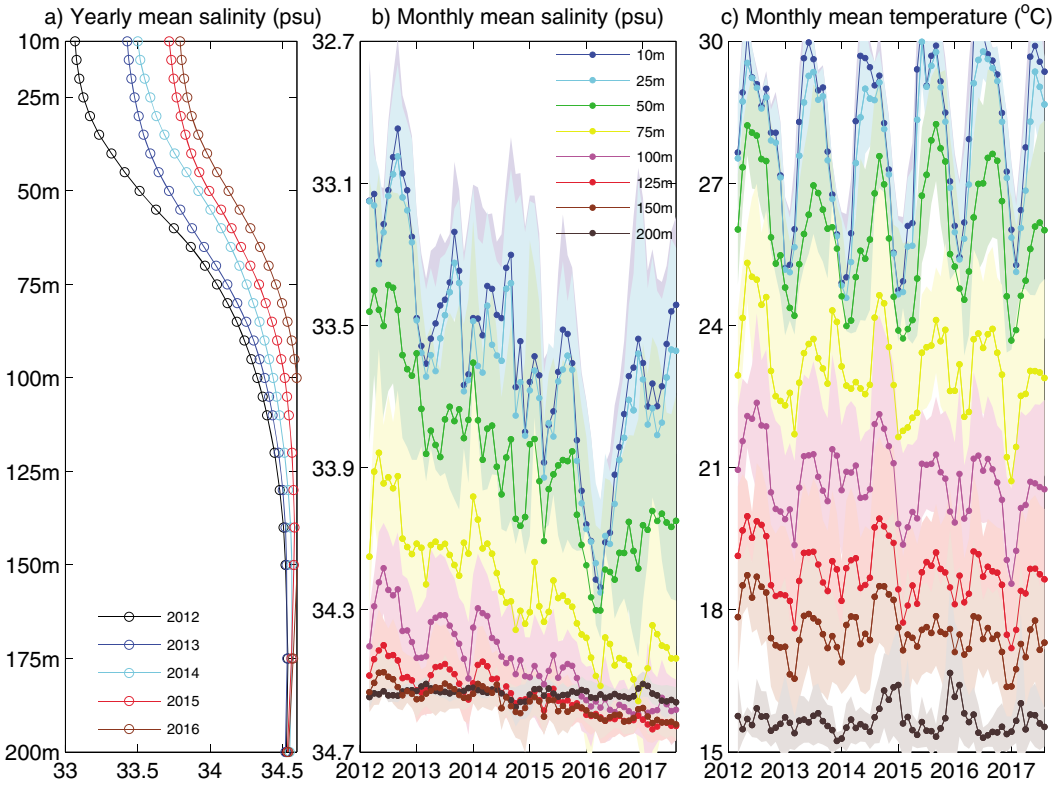

Figure 3. Vertical distributions of basin-average (a) yearly mean salinity from 2012 to 2016, (b) monthly mean salinity (lines and light shading indicated error bars), and (c) temperature in the upper 200 m from 2012 to September 2017.

what has been observed in the northwest Pacific, east of the Luzon Strait. This implies that the horizontal advection of salt from outside the SCS might not be the only determinant for the salinification in the SCS as surmised by Nan et al. (2013), who reported a weakening trend of the Kuroshio intrusion and thought that it was related to the freshening in the northeastern SCS in the 1990s and 2000s.

To determine as to whether the salinification occurs in any particular month, histograms of monthly box-average mean salinity are shown for the years 2012 to 2016 in Figure 2b. Significant seasonal variation with high salinity during spring and winter and low salinity during summer and autumn has been well documented previously (Zeng et al., 2014). The salinification trend is robust all year round although it is a little weaker during autumn (Figure S3). Note that the waters became much saltier in the spring of 2016, which we attribute to the evolution of the PDO (see discussion in section 3.2).

Is this salinification signal limited to the near-surface waters? Figure 3a illustrates the vertical distributions of the yearly mean salinity. The salinification signal since 2012 is strongest near the surface and decreases downward. Within the mixed layer (about 50 m) (Zeng, Wang, Chen, et al., 2016), the rate of increase reduces relatively slowly, while below the mixed layer, the salinification signal weakens rapidly. The overall increase is more evident in the time series of monthly mean salinity at different depths (Figure 3b). Also shown are the standard errors estimated for each month and each depth. The salinification is much greater above 50 m. At 150 m, there is only a slight increase, and at 200 m the salinity is almost constant. That is, to say, the intense salinification has spread from the surface to 150 m since late 2012. The temperature (Figure 3c), however, exhibits no significant change. This may be associated with the global warming "hiatus" from the 21st century (Kosaka & Xie, 2013).

3.2. What Contributes to the Salinification?

We next consider the causes of this salinification. As the largest marginal sea in the northwest Pacific Ocean, the SCS is influenced by the large-scale climate patterns in the PDO and the El Niño–Southern Oscillation (Deng et al., 2013; D. Wang et al., 2002; C. Wang, Wang, et al., 2006; Yu & Qu, 2013). Although the effect of

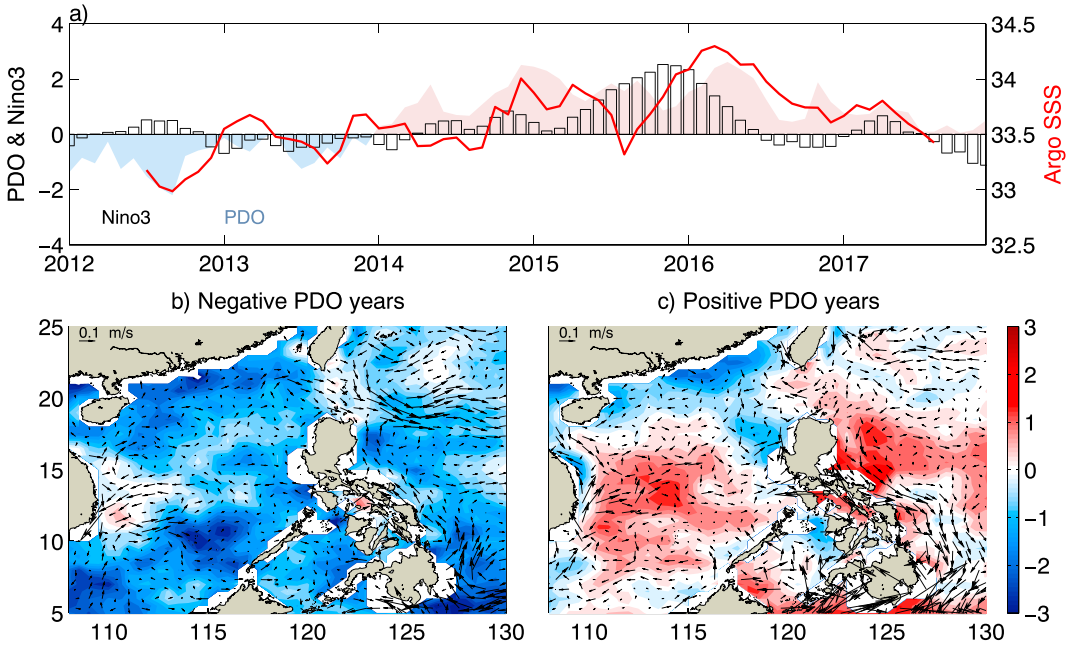

Figure 4. (a) Time series of the monthly Pacific Decadal Oscillation (PDO) index (shading; positive phase: red; negative phase: blue) and Niño3 (black bar) index from 2012 to 2017, and basin-average surface salinity Argo floats (red line) from July 2012 to September 2017. The freshwater flux anomaly (evaporation minus precipitation, shading, mm/d) and near-surface circulation anomaly (black vectors, m/s) in (b) negative (2012 and 2013) and (c) positive (2014, 2015 and 2016) PDO years. SSS = sea surface salinity.

the strong 2015/2016 El Niño event cannot be ignored, the change in Argo SSS during 2015 and 2016 is more closely correlated with the PDO, which reaches a maximum in spring 2016 when the 2015/2016 El Niño is decaying. From 2012 to the present, the PDO index has switched from negative to positive phase. The change of SSS agrees better with the evolution of the PDO than with the Niño3 index. Correlation coefficients between monthly SSS and the PDO (Niño3) index are 0.73 (0.27). This close relationship between SSS and PDO variability is further confirmed when extending the time series to the 1960s (Figure S4).

Previous studies have suggested that the impacts of PDO induce dry sinking air along with reduced precipitation in the SCS in the positive phase and the opposite situation in the negative phase (Krishnamurthy & Krishnamurthy, 2014). To examine the impact of different PDO phases in this region, the composite net surface freshwater flux (evaporation minus precipitation, positive values indicate net freshwater loss from the ocean) and ocean circulation in negative and positive PDO years are shown in Figures 4b and 4c, respectively. In contrast to the much wetter conditions during negative PDO phases, the SCS becomes drier during positive phases. In addition, the horizontal current also switched from eastward to westward through the Luzon Strait, leading to the advection of more salty water into the SCS in positive PDO phases than in negative phases.

To get a better view of the changes in the air-sea flux and oceanic advection, the differences of net surface freshwater flux and ocean circulation in the SCS between 2016 and 2012 are shown in Figure 5a. The freshwater flux loss was significantly larger in 2016 than in 2012 over most basin, except in the northeastern and west boundary regions. The linear trends of monthly freshwater flux from 2012 to 2016 are also calculated (Figure 5b). There is increased net freshwater loss in the SCS that has a similar spatial pattern to the difference field in Figure 5a. The net freshwater flux in the SCS is dominated by the precipitation. The comparison between precipitation evaporation is shown in Figure 5c. The latitude-time diagrams of the 109–121°E averaged net freshwater flux clearly show the increasing net freshwater loss from the SCS (Figure S5a).

In addition to the contrast in net freshwater flux, a trend of anomalous westward flow east of the Luzon Strait and into the basin is also evident from both monthly OSCAR (Figure 5b) and HYCOM reanalysis outputs (Figure S6). An anomalous westward flow intruded into the SCS, indicative of a stronger Kuroshio intrusion or Luzon Strait transport in 2015 than in 2012. This anomalous westward transport may lead to more high-salinity water entering the basin through the Luzon Strait driven by the SCS throughflow (D. Wang, Liu, et al., 2006; Xiao et al., 2017; Yu & Qu, 2013). The latitude-time diagrams zonal current within the

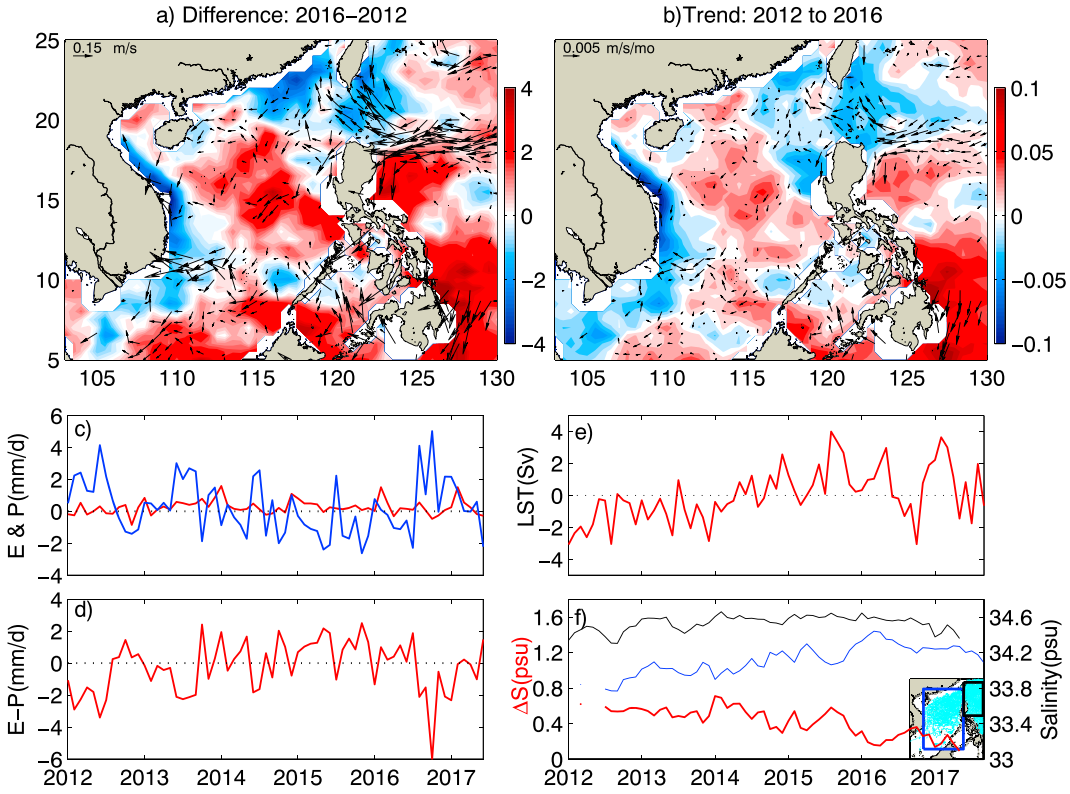

Figure 5. (a) The difference of freshwater flux (evaporation minus precipitation, shading, mm/d) and near-surface circulation (black vectors: westerly currents, m/s) between 2016 and 2012. (b) Linear trend of freshwater flux (shading, unit: mm/d/yr) and near-surface circulation from 2012 to 2016 (black vectors: unit: m/s/yr). Monthly time series of (c) evaporation anomaly (red curve, unit: cm/d) and precipitation anomaly (blue curve, unit: cm/d), and (d) net freshwater flux averaged over the South China Sea (109–121°E, 3–23°N) from 2012 to June 2017. Monthly time series of (e) Luzon Strait transport anomaly (Sv) and (f) salinity averaged within regions east of the Luzon Strait (121–127°E, 15–25°N, black curve) and the South China Sea (109–121°E, 3–23°N, blue curve), and the salinity difference between these two regions averaged in upper 150 m from Argo (red curve). Locations of the Argo floats and two selected areas used for spatial averages are shown in the inset.

Luzon Strait clearly illustrates the widening and strengthening intrusion into the SCS (Figure S5b). The monthly time series of Luzon Strait transport does show a rising tendency (Figure 5e).

Figure 6a shows basin-average net freshwater flux anomaly (evaporation anomaly minus precipitation anomaly) and salt transport anomaly into the basin across the Luzon Strait (defined as T_{LS}·ΔS), where positive values indicate net salt transported into the SCS and vice versa. Here T_{LS} is the Luzon Strait transport calculated from HYCOM reanalysis outputs; ΔS is the salinity difference between the regions east of the Luzon Strait and the SCS based on measurements of Argo floats. The time series of salinity averaged within these two regions and ΔS derived from Argo are shown in Figure 5f). There is an increase in the net freshwater loss and in the horizontal salt transport into the basin through the Luzon Strait, together providing favorable conditions for salinification from 2012 to the present. By comparing the variations of Luzon Strait transport, we can know that the enhanced salt transport is dominated by increased transport but not decreased salinity difference inside and outside of the basin.

To understand the relative importance of surface freshwater forcing and horizontal salinity advection through the Luzon Strait on the salinification, a diagnosis of the salinity anomalies they induce in the top 0–150 m is presented in Figure 6b. The contribution of surface freshwater forcing is calculated as $\Delta(E–P–R)\cdot S_0/H$, where $\Delta(E–P–R)$ is the freshwater anomaly relative to climatological monthly mean values, S_0 is the monthly mean near-surface salinity averaged above 10 m, and H is 150 m. The influence of river runoff shows that its contribution is much smaller than net freshwater flux (Figure S7). The horizontal advection term is simplified to $T_{LS} \cdot \Delta S/V_{scs}$, where $T_{LS} \cdot \Delta S$ is the salt transport through the Luzon Strait above 150 m and V_{scs} is the volume of the SCS above 150 m. The result shows that the combined contribution of surface freshwater forcing and horizontal advection term can basically explain the salinification except some heavy rain months in

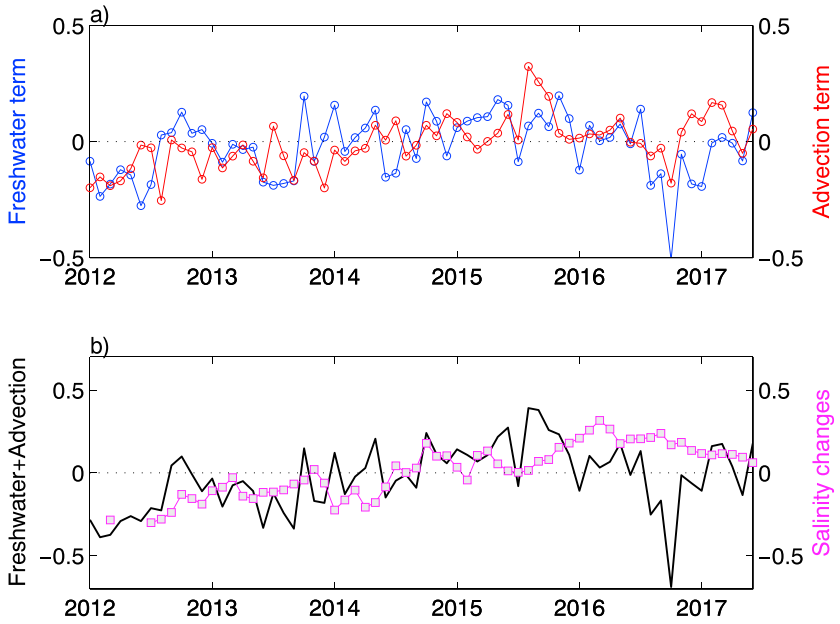

Figure 6. (a) Spatial average of surface freshwater forcing term (blue, psu/yr) and horizontal advection term in the upper 150 m (red) during 2012 to June 2017. (b) Changes of the upper 150 m salinity (magenta), and the sum of the freshwater term and horizontal advection term (black).

2016. Note that the enhancement in net freshwater loss and enhancement in horizontal salt transport are mainly caused by reduced precipitation (Figures 5c and 5d) and Luzon Strait transport, respectively (Figure 5ef). That is, sharp fall in precipitation and enhanced Luzon Strait transport dominated the current intense salinification.

4. Conclusion

A significant salinification is taking place in the SCS starting from late 2012 to the present, as seen in Aquarius/SMAP and Argo float data. The temperature, in contrast, exhibits no significant change. The salinification is strongest in the near-surface waters, of which the salinity increases from a minimum of 32.98 psu in September 2012 to a maximum of 34.30 psu in March 2016. The salinification signal spreads from the near-surface downward to 150 m, weakening sharply below the mixed layer.

The salinification is mainly associated with switches in the PDO from negative to positive phase from late 2012 to the present. A high correlation coefficient between the SSS and PDO confirms the major effect of the PDO on this salinification. The composite freshwater and horizontal circulation in negative and positive PDO phases shows that the SCS lost much more freshwater (dominated by reduced precipitation) and received more high-salinity water transported through the Luzon Strait in positive PDO phases than in negative phases. Changes of the freshwater fluxes and the horizontal circulation further show the increase in freshwater loss and salty water intrusion from 2012 to the present.

To better understand the causes of this salinification, we used a budget analysis that shows the combined contribution of surface freshwater forcing and the horizontal advection term. The combined contribution explains the most of the salinification, with exception for some heavy rain months, such as in October 2016 (Figure S8). Further studies and more data are needed to understand these events.

After a freshening period that lasted 20 years (1993–2012), we are particularly interested in whether the salinification that has been occurring since 2012 will continue in the future. Will the salinity continue to increase until it reaches at least the previous maximum observed in 1992? Another question that needs further study is the combined effect of a strong El Niño in a positive PDO phase on the salinity increase in the SCS. To answer such questions, we need to focus on subsequent observations, especially from Argo floats and from new salinity satellites.

Acknowledgments
Highly detailed comments and excellent revision suggestions from two anonymous reviews are gratefully acknowledged. We benefited from numerous data sets made freely available: OAFlux evaporation (ftp://ftp.whoi.edu/pub/science/oaflux/data_v3), TRMM 3B43 precipitation (http://mirador.gsfc.nasa.gov/cgi-bin/mirador/), OSCAR currents (http://podaac.jpl.nasa.gov/dataset/OSCAR_L4_OC_third-deg), HYCOM reanalysis outputs (http://hycom.org/dataserver/glb-reanalysis), PDO index (http://research.jisao.washington.edu/pdo/), and the Niño3 index (http://www.cpc.ncep.noaa.gov/data/indices/). This research has been supported by the Major State Research Development Program of China (2016YFC1402603) and the National Natural Science Foundation of China (41776025, 41476014, 41776026, and 41676018). E. P. C. and X. X. acknowledge the support of NOAA Climate Program Office MAPP Program (award NA15OAR4310088) and the National Science Foundation Physical Oceanography Program (award 1537136). R. W. S. was supported by NSF grant ICER-1663704. L. Z. is also sponsored by the Pearl River S&T Nova Program of Guangzhou and the Open Project Program of State Key Laboratory of Tropical Oceanography (LTOZZ1601).

References

Argo (2000). Argo float data and metadata from Global Data Assembly Centre (Argo GDAC). SEANOE. https://doi.org/http://doi.org/10.17882/42182

Bonjean, F., & Lagerloef, G. S. E. (2002). Diagnostic model and analysis of the surface currents in the tropical Pacific Ocean. *Journal of Physical Oceanography*, *32*(10), 2938–2954. https://doi.org/10.1175/1520-0485(2002)032%3C2938:DMAAOT%3E2.0.CO;2

Chassignet, E. P., Hurlburt, H. E., Metzger, E. J., Smedstad, O. M., Cummings, J., Halliwell, G. R., et al. (2009). U.S. GODAE: Global ocean prediction with the HYbrid Coordinate Ocean Model (HYCOM). *Oceanography*, *22*(2), 64–75. https://doi.org/10.5670/oceanog.2009.39

Cheng, X., Xie, S. P., Du, Y., Wang, J., Chen, X., & Wang, J. (2016). Interannual-to-decadal variability and trends of sea level in the South China Sea. *Climate Dynamics*, *46*(9–10), 3113–3126.

Curry, R., Dickson, B., & Yashayaev, I. (2003). A change in the freshwater balance of the Atlantic Ocean over the past four decades. *Nature*, *426*(6968), 826–829. https://doi.org/10.1038/nature02206

Delcroix, T., Cravatte, S., & McPhaden, M. J. (2007). Decadal variations and trends in tropical Pacific sea surface salinity since 1970. *Journal of Geophysical Research*, *112*, C03012. https://doi.org/10.1029/2006JC003801

Deng, W., Wei, G., Xie, L., Ke, T., Wang, Z., Zeng, T., & Liu, Y. (2013). Variations in the Pacific Decadal Oscillation since 1853 in a coral record from the northern South China Sea. *Journal of Geophysical Research: Oceans*, *118*, 2358–2366. https://doi.org/10.1002/jgrc.20180

Du, Y., Zhang, Y., Feng, M., Wang, T., Zhang, N., & Wijffels, S. (2015). Decadal trends of the upper ocean salinity in the tropical Indo-Pacific since mid-1990s. *Scientific Reports*, *5*, 16050. https://doi.org/10.1038/srep16050

Durack, P. J., & Wijffels, S. E. (2010). Fifty-year trends in global ocean salinities and their relationship to broad-scale warming. *Journal of Climate*, *23*(16), 4342–4362. https://doi.org/10.1175/2010JCLI3377.1

Durack, P. J., Wijffels, S. E., & Matear, R. J. (2012). Ocean salinities reveal strong global water cycle intensification during 1950 to 2000. *Science*, *336*(6080), 455–458. https://doi.org/10.1126/science.1212222

Fore, A. G., Yueh, S. H., Tang, W., Stiles, B., & Hayashi, A. K. (2016). Combined active/passive retrievals of ocean vector wind and sea surface salinity with SMAP. *IEEE Transactions on Geoscience and Remote Sensing*, *54*(12), 7396–7404. https://doi.org/10.1109/TGRS.2016.2601486

Huffman, G. J., Adler, R. F., Bolvin, D. T., Gu, G., Nelkin, E. J., Bowman, K. P., et al. (2007). The TRMM multisatellite precipitation analysis: Quasi-global, multi-year, combined-sensor precipitation estimates at fine scale. *Journal of Hydrometeorology*, *8*(1), 38–55. https://doi.org/10.1175/JHM560.1

Kosaka, Y., & Xie, S. P. (2013). Recent global-warming hiatus tied to equatorial Pacific surface cooling. *Nature*, *501*(7467), 403–407. https://doi.org/10.1038/nature12534

Krishnamurthy, L., & Krishnamurthy, V. (2014). Influence of PDO on South Asian summer monsoon and monsoon–ENSO relation. *Climate Dynamics*, *42*(9–10), 2397–2410. https://doi.org/10.1007/s00382-013-1856-z

Lagerloef, G., Boutin, J., Carton, J., Chao, Y., Delcroix, T., Font, J., et al. (2010). Resolving the global surface salinity field and variations by blending satellite and in situ observations. In J. Hall, D. E. Harrison, & D. Stammer (Eds.), *Proceedings of OceanObs'09: Sustained Ocean Observations and Information for Society* (Vol. 2), Venice, Italy: ESA Publication WPP-306, 21–25 September 2009.

Lagerloef, G., Wentz, F., Yueh, S. H., Kao, H., Johnson, G., & Lyman, J. (2012). Aquarius satellite mission provides new, detailed view of sea surface salinity, in state of the climate in 2011, B. *American Meteorological Society*, *93*(7), S70–S71.

Munk, W. (2003). Ocean freshening, sea level rising. *Science*, *300*(5628), 2041–2043. https://doi.org/10.1126/science.1085534

Nan, F., Xue, H., Chai, F., Wang, D., Yu, F., Shi, M., et al. (2013). Weakening of the Kuroshio intrusion into the South China Sea over the past two decades. *Journal of Climate*, *26*(20), 8097–8110. https://doi.org/10.1175/JCLI-D-12-00315

Nyadjro, E. S., Subrahmanyam, B., & Giese, B. S. (2013). Variability of salt flux in the Indian Ocean during 1960–2008. *Remote Sensing of Environment*, *134*, 175–193. https://doi.org/10.1016/j.rse.2013.03.005

Reul, N., Fournier, S., Boutin, J., Hernandez, O., Maes, C., Chapron, B., et al. (2014). Sea surface salinity observations from space with the SMOS satellite: A new means to monitor the marine branch of the water cycle. *Surveys in Geophysics*, *35*(3), 681–722. https://doi.org/10.1007/s10712-013-9244-0

Roemmich, D., Belboch, M., Freeland, H., Garzoli, S. L., John, G. W., Grant, F., et al. (2009). Argo: The challenge of continuing 10 years of progress. *Oceanography*, *22*(3), 46–55. https://doi.org/10.5670/oceanog.2009.65

Rong, Z., Liu, Y., Zong, H., & Cheng, Y. (2007). Interannual sea level variability in the South China Sea and its response to ENSO. *Global and Planetary Change*, *55*(4), 257–272. https://doi.org/10.1016/j.gloplacha.2006.08.001

Schmitt, R. W. (2008). Salinity and the global water cycle. *Oceanography*, *21*(1), 12–19. https://doi.org/10.5670/oceanog.2008.63

Schmitt, R. W., & Blair, A. (2015). A river of salt. *Oceanography*, *28*(1), 40–45. https://doi.org/10.5670/oceanog.2015.04

Skliris, N., Marsh, R., Josey, S. A., Good, S. A., Liu, C., & Allan, R. P. (2014). Salinity changes in the World Ocean since 1950 in relation to changing surface freshwater fluxes. *Climate Dynamics*, *43*(3–4), 709–736. https://doi.org/10.1007/s00382-014-2131-7

Wang, D., Xie, Q., Du, Y., Wang, W., & Chen, J. (2002). The 1997–1998 warm event in the South China Sea. *Chinese Science Bulletin*, *47*(14), 1221–1227.

Wang, C., Wang, W., Wang, D., & Wang, Q. (2006). Interannual variability of the South China Sea associated with El Niño. *Journal of Geophysical Research*, *111*, C03023. https://doi.org/10.1029/2005JC003333

Wang, D., Liu, Q., Huang, R. X., Du, Y., & Qu, T. (2006). Interannual variability of the South China Sea throughflow inferred from wind data and an ocean data assimilation product. *Geophysical Research Letters*, *33*, L14605. https://doi.org/10.1029/2006GL026316

Xiao, F., Zeng, L., Liu, Q. Y., Zhou, W., & Wang, D. (2017). Extreme subsurface warm events in the South China Sea during 1998/99 and 2006/07: Observations and mechanisms. *Climate Dynamics*, *50*(1-2), 115–128. https://doi.org/10.1007/s00382-017-3588-y

Yu, K., & Qu, T. (2013). Imprint of the Pacific Decadal Oscillation on the South China Sea throughflow variability. *Journal of Climate*, *26*(24), 9797–9805. https://doi.org/10.1175/JCLI-D-12-00785.1

Yu, L., & Weller, R. A. (2007). Objectively analyzed air-sea heat fluxes for the global ice-free oceans (1981–2005). *Bulletin of the American Meteorological Society*, *88*(4), 527–540. https://doi.org/10.1175/BAMS-88-4-527

Zeng, L., Liu, W. T., Xue, H., Xiu, P., & Wang, D. (2014). Freshening in the South China Sea during 2012 revealed by Aquarius and in situ data. *Journal of Geophysical Research: Oceans*, *119*, 8296–8314. https://doi.org/10.1002/2014JC010108

Zeng, L., Wang, D., Xiu, P., Shu, Y., Wang, Q., & Chen, J. (2016). Decadal variation and trends in subsurface salinity from 1960 to 2012 in the northern South China Sea. *Geophysical Research Letters*, *43*, 12,181–12,189. https://doi.org/10.1002/2016GL071439

Zeng, L., Wang, D., Chen, J., Wang, W., & Chen, R. (2016). SCSPOD14, a South China Sea physical oceanographic dataset derived from in situ measurements during 1919–2014. *Science Data*, *3*, 160029. https://doi.org/10.1038/sdata.2016.29